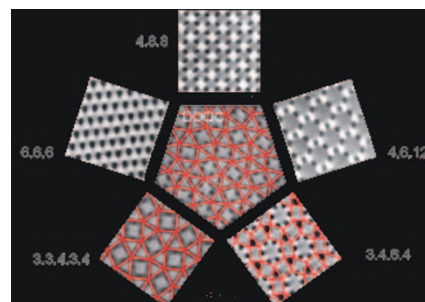


AWARD ACCOUNTS

SPSJ Award Accounts

Precise Molecular Design of Complex Polymers and Morphology Control of Their Hierarchical Multiphase Structures

Three arm star polymers of the $I_XS_YP_Z$ type composed of polyisoprene (I), polystyrene (S) and poly(2-vinylpyridine) (P) with different compositions were anionically prepared. Their solvent-cast and annealed bulk films exhibited cylinder-assembled ordered structures whose cross-sections represent two-dimensional tiling patterns. Most of them can be characterized as the Archimedean tiling patterns, while a polymer with composition of $I_{1.0}S_{2.7}P_{2.5}$ exhibits dodecagonal quasicrystalline (DDQC) structure with mesoscopic length scale.

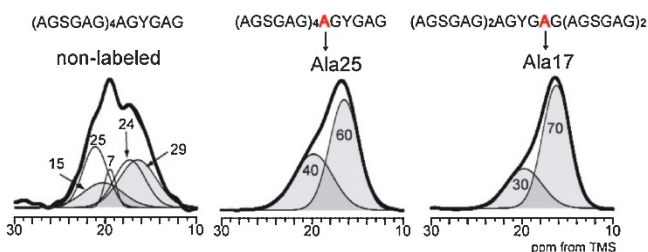


Y. MATSUSHITA
Vol. 40, No. 3, pp 177–183 (2008)

SHORT COMMUNICATION

The Influence of Ser and Tyr Residues on the Structure of *Bombyx Mori* Silk Fibroin Studied Using High-resolution Solid-state ^{13}C NMR Spectroscopy and ^{13}C Selectively Labeled Model Peptides

In order to examine the influence of Ser and Tyr residues in silk II structure of *B. mori* silk fibroin, we synthesized several ^{13}C selectively labeled model peptides containing Ser and Tyr residues in $(\text{AG})_n$, mimicking the primary structure of *B. mori* silk fibroin. The ^{13}C CP/MAS NMR spectra indicated that the presence of Ser residue promoted silk II structure, but Tyr residue destroyed silk II structure largely depending on the position of the introduction in the chain.

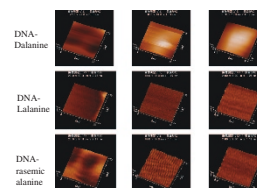


H. SATO, M. KIZUKA, Y. NAKAZAWA, and T. ASAKURA
Vol. 40, No. 3, pp 184–185 (2008)

REGULAR ARTICLE

DNA–Lipid Hybrid Films Derived from Chiral Lipids

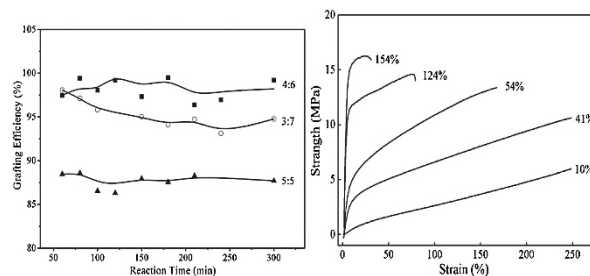
DNA-L-alanine C10 film exhibited an uneven surface with a regular interval pattern



N. OGATA and K. YAMAOKA
Vol. 40, No. 3, pp 186–191 (2008)

High Efficient Grafting Polymerization of Styrene on Surface of NBR Latex and Physical Properties of NBR/NBR-g-PSt Composite

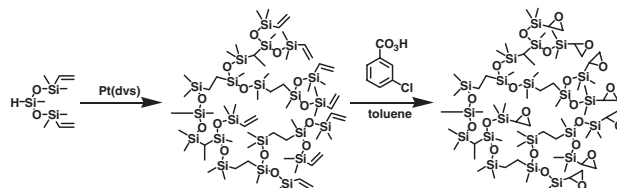
Commercial available vulcanized acrylonitrile butadiene rubber (NBR) latex was modified *via* grafting PSt on surface with high efficiency. Factors affinitive to the grafting polymerization were discussed. Morphologies of the thermal compression molded composites of NBR/NBR-g-PSt observed by TEM indicated that no phase agglomeration occurred during thermal process. Tensile behaviors test demonstrated that when the grafting yield was controlled at about 50%, the strength of modified rubbers increased significantly without losing its elongation.



Q. WANG, L. LIU, and W. YANG
Vol. 40, No. 3, pp 192–197 (2008)

Synthesis and Degree of Branching of Epoxy-Terminated Hyperbranched Polysiloxysilane

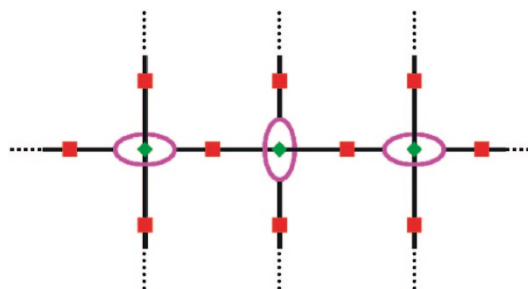
Hyperbranched polysiloxysilane (HBPS) with terminal vinyl groups was synthesized by self-condensation using platinum-catalyzed hydrosilylation of 1,1,3,5,5-pentamethyl-1,5-divinyltrisiloxane. End-functionalization of terminal vinyl groups was carried out by epoxidation with 3-chloroperoxybenzoic acid to afford epoxy-terminated HBPS. The degree of branching of HBPS was estimated as 0.57 in comparison of ^{29}Si NMR spectra of epoxy-terminated HBPS and the model compounds.



K. YOKOMACHI, M. SEINO, S. J. GRUNZINGER,
T. HAYAKAWA, and M. KAKIMOTO
Vol. 40, No. 3, pp 198–204 (2008)

Pseudorotaxane-coupled Gel: A New Concept of Interlocked Gel Synthesis by Using Metathesis Reaction

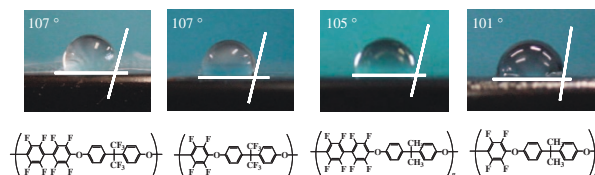
A unique interlocked gel consisting of an ammonium salt axle having two terminal olefins and a crown ether having two terminal olefins was synthesized by metathesis reaction of pseudorotaxane. The resulting compound showed a swelling in various solvents and showed no solubility.



K. YAMABUKI, Y. ISOBE, K. ONIMURA, and T. OISHI
Vol. 40, No. 3, pp 205–211 (2008)

Synthesis and Characterization of Polymers from Bisphenol Derivatives and Perfluorinated Aromatic Compounds

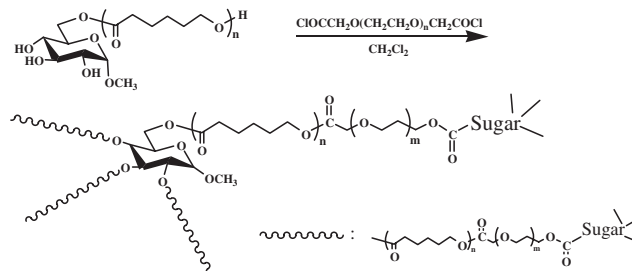
Polycondensation of perfluorobiphenyl or hexafluorobenzene with bisphenol-AF or bisphenol-A in the presence of NaH as base in DMAc gave polymers consisting of repeating units from I to IV. These fluoro-containing polymers showed a high decomposition temperature, T_g and high contact angles to water.



K. ENDO and T. YAMADE
Vol. 40, No. 3, pp 212–216 (2008)

Tailor-Made Amphiphilic Biodegradable Polymer-Gels: 1. Gel Preparation via Controlled Ring-opening Polymerization Using Glucopyranoside As Initiator and Subsequent Coupling with α,ω -Bifunctional PEG

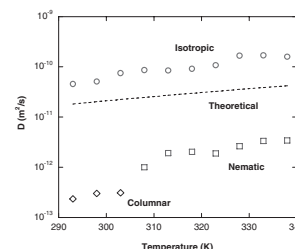
Novel amphiphilic and biodegradable gels composed of glucopyranoside, poly(ϵ -caprolactone) (PCL), and poly(ethylene glycol) (PEG) were synthesized. Methyl-2,3-di-*O*-benzyl- α -D-glucopyranoside was used as an initiator for ring-opening polymerization (ROP) of ϵ -caprolactone (ϵ -CL). The primary hydroxyl group (C6-OH) was effective as the initiation site for living ROP of ϵ -CL, and yielded sugar-headed PCL. Both termini of PEO chain were converted to α,ω -dicarboxylic chloride as a coupling reagent for the tailor-made gel having a sequence of “Sugar-PCL-PEG-PCL-Sugar.”



Y. MORIKAWA, H. KINOSHITA, M. ASAHI,
A. TAKASU, and T. HIRABAYASHI
Vol. 40, No. 3, pp 217–222 (2008)

Diffusional Behavior of Poly(γ -benzyl L-glutamate) in Concentrated Solution As Studied by the Field-Gradient ^1H NMR Methods

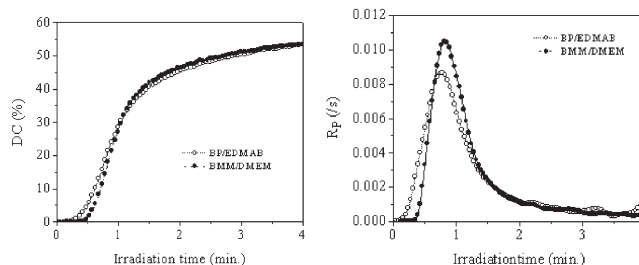
The diffusion coefficient (D) of poly(γ -benzyl L-glutamate) (PBLG) in the isotropic, nematic and columnar phases in concentrated solution is determined by the field-gradient ^1H NMR methods. The D values in the isotropic phase are a little bit larger than the identical calculated D values of a PBLG chain, which means PBLG chains move independently. Whereas the D values in other phases are smaller than the identical calculated D values of a PBLG chain. It means several PBLG chains move cooperatively.



S. KUROKI and K. KAMIGUCHI
Vol. 40, No. 3, pp 223–227 (2008)

Synthesis and Evaluation of 4-Benzophenone Methoxyl Methacrylate As a Polymerizable Photoinitiator

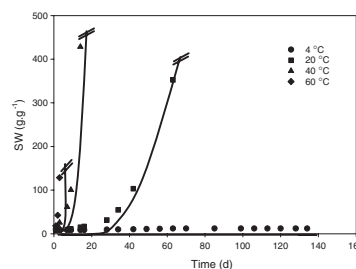
4-Benzophenone methoxyl methacrylate (BMM)/2-(*N,N*-dimethylamino) ethylmethacrylate (DMEM) system and benzophenone (BP)/ethyl 4-(dimethylamino)benzoate (EDMAB) system could reach the same double conversion for 4 min exposure. Compared with the nonpolymerizable initiator system (BP/EDMAB), BMM/DMEM led to slightly higher maximum R_p , which meant that the reactivity of BMM/DMEM was relatively higher than that of BP/EDMAB in the same curing condition.



G. HOU, S. SHI, S. LIU, and J. NIE
Vol. 40, No. 3, pp 228–232 (2008)

Metastable Amphiphilic Hydrogels Based on Cross-linked Carboxymethylpullulan

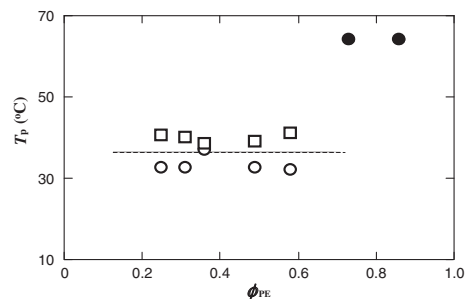
Amphiphilic hydrogels obtained by crosslinking of Carboxymethylpullulan and dibromohexan exhibit a transition gel/sol dependent of time and temperature. Initial percolation of these hydrogels was obtained by coexistence of chemical links and hydrophobic associations. The metastable behavior is due to reorganization of hydrophobic associations.



M. LEGROS, P. CARDINAEL, V. DULONG,
L. PICTON, and D. LE CERF
Vol. 40, No. 3, pp 233–240 (2008)

Composition Dependence of Crystallization Behavior Observed in Crystalline-Crystalline Diblock Copolymers

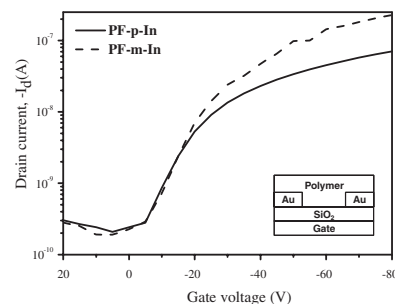
The crystallization behavior of poly(ϵ -caprolactone) (PCL) blocks starting from a solid morphology formed in advance by the crystallization of polyethylene (PE) blocks in PCL-*b*-PE copolymers has been investigated by time-resolved synchrotron small-angle X-ray scattering as a function of composition (or volume fraction of PE blocks ϕ_{PE} in the system). The temperature T_p at which the crystallization mechanism of PCL blocks changed was almost independent of ϕ_{PE} for PCL-*b*-PE with $\phi_{PE} \leq 0.58$. However, the PE block crystallized within molten microdomains for PCL-*b*-PE with $\phi_{PE} \geq 0.73$, by which the crystallization of PCL blocks was completely confined at every T_c .



H. IKEDA, Y. OHGUMA, and S. NOJIMA
Vol. 40, No. 3, pp 241–248 (2008)

Synthesis of New Fluorene-Indolocarbazole Alternating Copolymers for Light-Emitting Diodes and Field Effect Transistors

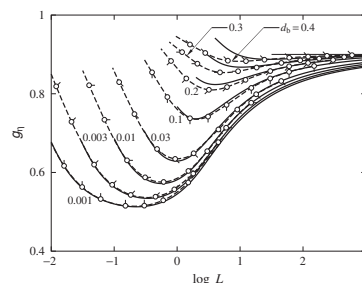
New fluorene-indolocarbazole alternating copolymers of para-linkage **PF-p-In** and meta-linkage **PF-m-In** were synthesized and characterized for light-emitting diodes and field effect transistors (FET). The para-linkage **PF-p-In** has a lower optical band gap and higher emission maximum than those of **PF-m-In**. The electroluminescence characteristics of **PF-p-In** and **PF-m-In** show similar maximum luminance characteristics but different emissive colors of blue and green, respectively. The FET hole mobilities of **PF-p-In** and **PF-m-In** are significantly higher than that of polyfluorene.



W.-Y. LEE, C.-W. CHEN, C.-C. CHUEH, C.-C. YANG, and W.-C. CHEN
Vol. 40, No. 3, pp 249–255 (2008)

Intrinsic Viscosity of Wormlike Regular Three-Arm Stars

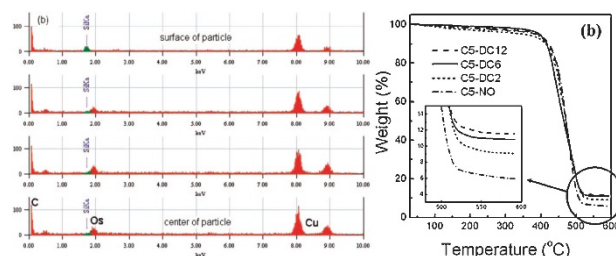
The ratio g_η of the intrinsic viscosity of the Kratky–Porod (KP) wormlike regular three-arm star touched-bead model to that of the KP linear one, both having the same (reduced) total contour length L and (reduced) bead diameter d_b , is evaluated in the Kirkwood–Riseman approximation, and its behavior as a function of L and d_b is examined (unfilled circles). An empirical interpolation formula for g_η (solid curves) is also proposed.



D. IIDA, Y. NAKAMURA, and T. YOSHIZAKI
Vol. 40, No. 3, pp 256–267 (2008)

Effect of Reactive Amphiphiles on the Silicate Dispersion and Degradation Behavior of ABS/layered Silicate Nanocomposites

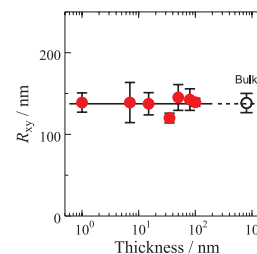
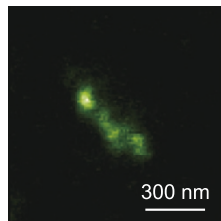
The dispersion of silicate in ABS/silicate nanocomposites depended on the hydrophobic chain lengths of reactive amphiphiles. The silicates are exfoliated and dispersed homogeneously on the surfaces of ABS/silicate nanocomposites as certified by TEM image and EDAX analysis. The nanocomposite obtained by using DC12 produced a slightly larger amount of residue than those by DC2 and DC6 and its decomposition temperature was also higher.



J. H. KIM, K. KIM, Y. C. KIM, and I. J. CHUNG
Vol. 40, No. 3, pp 268–273 (2008)

Conformation of Single Poly(methyl methacrylate) Chains in an Ultra-Thin Film Studied by Scanning Near-Field Optical Microscopy

The conformation of a poly(methyl methacrylate) chain in an ultra-thin film is discussed by the direct observation of the individual chains using scanning near-field optical microscopy. We examined the effect of the spatial constraint in the thin film on the chain dimension in the film plane, R_{xy} . In the thickness range of 1–100 nm, R_{xy} in an ultra-thin film was not significantly altered from that in the bulk state, indicating that the lowered interchain entanglement in the ultra-thin film.



H. AOKI, S. MORITA, R. SEKINE, and S. ITO
Vol. 40, No. 3, pp 274–280 (2008)